Investigating the Interaction between SARS-CoV-2 NSP15 and a Human E3 Ubiquitin Ligase Using In Silico Methods

Annika Viswesh[1], Soichi Wakatsuki[2]
[1]Palo Alto High School (Palo Alto, CA, United States)
[2]Department of Structural Biology, Stanford University (Stanford, CA, United States)

Abstract

Patients with acute respiratory distress due to SARS-CoV-2 infection exhibit hyper-inflammatory response and Type 1 Interferon (IFN-1) deficiency. Recent studies indicate that SARS-CoV-2 NSP15 suppresses the immune response; however, this has not been investigated at a molecular level. RNF41, a human E3 ubiquitin ligase, controls inflammation and IFN-1 production by binding to MYD88 and TBK1 in the immune signaling pathways. We hypothesized that SARS-CoV-2 NSP15 binds to RNF41 and inhibits RNF41 from regulating the immune signaling pathways. Molecular docking of RNF41 C-terminal domain (CTD) to five NSP15 poses, MYD88, TBK1, and USP8, were each performed, and binding residues with distances <= 3 Å were measured. Previously unknown structure of RNF41 Zinc-finger domain (ZFD) was generated using homology modeling. Previously unknown active sites on RNF41 ZFD were determined by developing computational algorithms to explore ~170,000 structures in PDB with a structural alignment score of < 2 Å and having zinc finger motifs with complexes. The resulting sites were used to dock RNF41 ZFD to five NSP15 poses. Results showed that NSP15, TBK1, MYD88, and USP8 bound to the same residues of RNF41 CTD. NSP15 had the highest binding affinity to RNF41 CTD. RMSD plots of MD simulations indicated that the RNF41-NSP15 complex reached stability of ~0.51 nm at 7 ns. RMSF of 83% of the binding residues was lower than average fluctuations indicating high stability. The preliminary MD simulations so far support the docking results. This confirmed our hypothesis that binding between RNF41 CTD and NSP15 could cause the immune system's disruption. Further, NSP15's binding sites were located > ~8 Å away from its catalytic site, indicating that NSP15's cleaving function could continue even when NSP15 binds to RNF41 CTD. These results set the direction for researching drugs to target SARS-CoV-2 NSP15's binding sites.

Normal cell

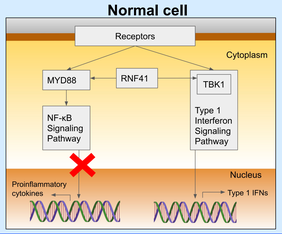

SARS-CoV-2 infected cell

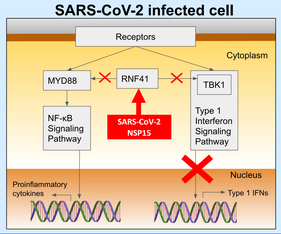

Methods

Investigate binding to RNF41 CTD

1. Build hexamer structure of NSP15 from the dimer(6VWW) downloaded from the PDB
2. Perform docking of RNF41 to USP8, RNF41 to TBK1, RNF41 to MYD88, and RNF41 to different poses of NSP15
3. Choose the best docking using the metrics of haddock score, number of clusters, and members in each cluster
4. Extract binding sites with binding distances <= 3.5 Å

Investigate binding to RNF41 ZFD

1. Use Homology Modeling to generate unknown structure of RNF41 ZFD
2. Develop computational algorithm to filter structurally similar proteins based on the following criteria:
   i. Align Score < 2 Å RMSD after structurally aligning with RNF41 ZFD
   ii. CYS-CYS-HIS-HIS Zinc motifs within 3 Å of each other and docked to another protein with the complex available in the PDB.
3. Determine active binding sites sites on RNF41 ZFD by finding active binding sites on structurally similar resulting proteins.
4. Perform docking between RNF41 ZFD and NSP15
5. Select best docking, find binding sites, and measure binding distances

Investigate stability of the docked structure with top docking scores

1. Perform Molecular Dynamics (MD) Simulations and analyze metrics

Generating NSP15 hexamer from dimer

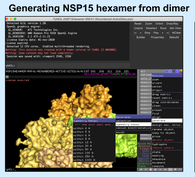

Sequence of RNF41 showing the location of different domains

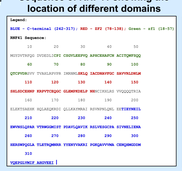

RNF41 ZFD generated by sequence comparisons and Homology modeling

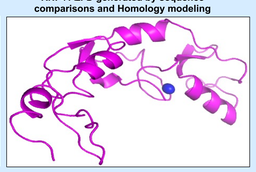

Results and Discussion

Docking results of USP8 and RNF41 CTD

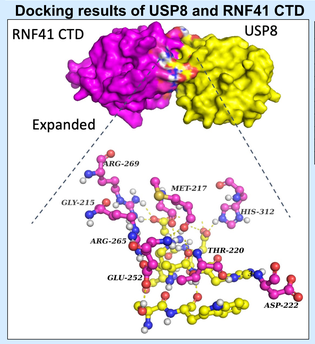

Binding sites of USP8 and RNF41 CTD

type	RNF41= chain_a	USP8= chain_b	resname_a	resname_b	resid_a	resid_b	atom_a	atom_b	Distances
ionic	A	B	ARG	ASP	265	241	NE	OD2	2.7
ionic	A	B	ARG	ASP	269	242	NH2	OD1	2.6
ionic	A	B	GLU	LYS	252	244	OE1	NZ	3.1
hbond	A	B	THR	ALA	220	237	OG1	O	2.7
hbond	A	B	GLN	ASP	266	242	NE2	OD1	3.4
hbond	A	B	MET	ASP	217	241	O	N	2.7
hbond	A	B	GLY	ASP	215	242	O	N	3.2
hbond	A	B	HIS	GLN	312	211	NE2	OE1	3.8
hbond	A	B	ASP	HIS	222	238	OD2	NE2	3.2
ionic	A	B	ARG	ASP	265	241	NH2	OD1	2.7

The previously known active binding sites of RNF41 are GLY-215, MET-217, THR-220, ASP-222, GLU-252, ARG-265, ARG-269, and HIS-312. Docking results matched previously published crystallization data results. This validated the choice of Haddock as a reliable docking server.

The binding energy (Haddock score) of the complex of USP8 and RNF41 was -75.8 +/- 6.6 which indicates a good binding affinity.

Docking results of TBK1 and RNF41 CTD

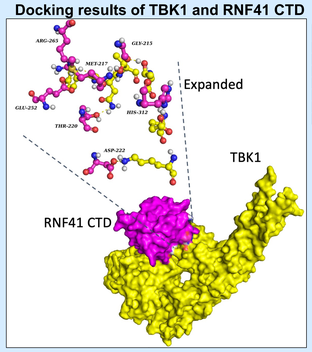

Binding sites of TBK1 and RNF41 CTD

type	chain_a = RNF41	chain_b = TBK1	resname_a	resname_b	resid_a	resid_b	atom_a	atom_b	Distances
hbond	A	B	GLY	SER	215	218	O	N	3.5
hbond	A	B	MET	SER	217	218	O	NZ	2.7
hbond	A	B	SER	GLU	219	219	OG	NE2	2.8
hbond	A	B	THR	GLU	220	219	OG1	N	2.5
ionic	A	B	ASP	LYS	222	220	OD1	NZ	1.8
hbond	A	B	GLU	HIS	252	158	OE2	NE2	3.3
hbond	A	B	HIS	ALA	312	102	NE2	O	1.8

Binding of RNF41 CTD to TBK1 matched 6 of 8 active sites on RNF41 CTD. The overlapping binding sites on RNF41 between TBK1 and USP8 were GLY-215, MET-217, THR-220, ASP-222, GLU-252, and HIS-312. The binding energy (Haddock score) of the complex of TBK1 and RNF41 was -75.0 +/- 8.8 which indicates a good binding affinity.

Docking results of MYD88 and RNF41 CTD

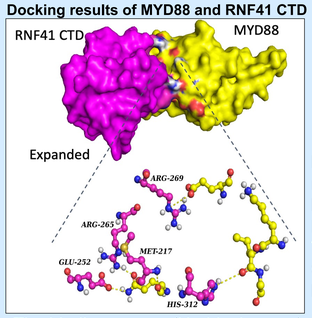

Binding sites of MYD88 and RNF41 CTD

type	RNF41= chain_a	MYD88= chain_b	resname_a	resname_b	resid_a	resid_b	atom_a	atom_b	Distances
ionic	A	B	ARG	GLU	269	52	NE	OE2	3.8
ionic	A	B	ARG	GLU	270	57	NE	OE2	2.8
hbond	A	B	ARG	LEU	213	96	NH1	O	2.9
hbond	A	B	ARG	LYS	213	95	NH2	O	3.4
hbond	A	B	ARG	GLN	265	42	NH2	OE1	2.8
hbond	A	B	GLN	GLU	266	65	NE2	OE1	2.8
hbond	A	B	GLU	GLU	252	42	OE2	NE2	2.9
hbond	A	B	MET	GLU	217	42	O	N	3.2
hbond	A	B	HIS	LEU	312	96	NE2	O	4

Binding of RNF41 CTD to MYD88 matched 5 of 8 active sites on RNF41 CTD. The overlapping binding sites on RNF41 between TBK1 and USP8 were MET-217, GLU-252, ARG-265, ARG-269, and HIS-312.

The binding energy (Haddock score) of the complex of MYD88 and RNF41 was -72.9 +/- 10.6 which indicates a good binding affinity.

Docking results of NSP15 and RNF41 CTD

Docking of 5 poses of NSP15 with RNF41 CTD resulted in docking pose 2 with greatest binding score. Discovered that it binds to **6 out of the 8 active sites** of RNF41 CTD

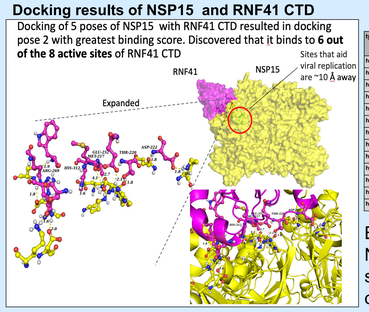

Binding sites of NSP15 pose#2 and RNF41 CTD

type	chain_a = RNF41	chain_b = NSP15	resname_a	resname_b	resid_a	resid_b	atom_a	atom_b	Distances
hbond	A	B	ASP	LYS	222	1566	OD2	NZ	1.8
hbond	A	B	ASP	GLU	222	1563	HN	O	1.8
hbond	A	B	THR	SER	220	242	HG1	O	1.8
hbond	A	B	GLU	HIS	252	243	OE2	HE2	2.1
hbond	A	B	ALA	ARG	311	258	O	HH11	2.7
hbond	A	B	HIS	GLU	312	261	HD1	OE1	1.6
hbond	A	B	HIS	GLU	312	261	HD1	OE2	2.2
hbond	A	B	GLN	GLU	266	340	HE22	OE1	2
hbond	A	B	GLU	LYS	263	335	OE1	HZ3	1.6
hbond	A	B	ARG	GLU	269	234	HH22	OE2	1.8
hbond	A	B	ARG	GLU	269	234	HE22	OE2	2.3
hbond	A	B	TRP	ASP	214	220	HN	OD2	1.9
hbond	A	B	MET	SER	217	242	O	OG	4.1

Binding of RNF41 CTD To NSP15 matched 6 of 8 active sites on RNF41 CTD. The overlapping binding sites on RNF41 between NSP15 pose#2 and USP8 were MET-217, THR-200, ASP-222, GLU-252, ARG-269, and HIS-312. The binding energy of the complex of NSP15 pose#2 and RNF41 was -110.9 +/- 3.6 which indicates a good binding affinity. RNF41 CTD docked to NSP15 pose#2 had best binding energy.

Results and Discussion

Algorithm to filter structurally similar proteins to RNF41 ZFD

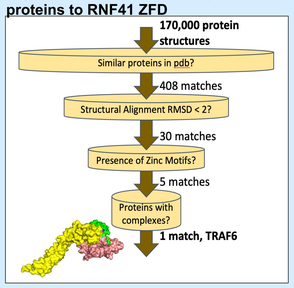

Determined the potential active sites on RNF41 ZFD using the binding sites of TRAF6. Docking of 5 poses of NSP15 with RNF41 ZFD resulted in docking pose #1 with greatest binding score of -64.4 +/- 7.0

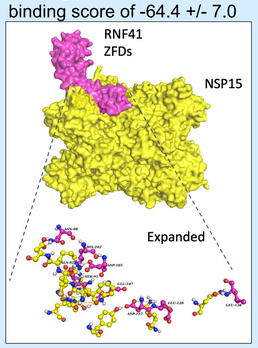

Computation algorithm performed extensive sequence comparisons with 170,000 protein structures in PDB and resulted in one similar protein, TRAF6.

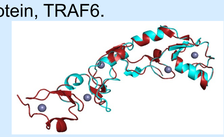

Alignment RMSD between RNF41 ZFD and TRAF6 was 0.15 Å, which indicated excellent structural similarity.

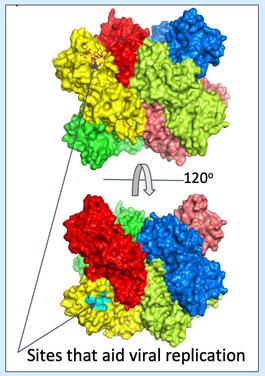

The sites on NSP15 responsible for viral replication are different from the binding sites for docking with RNF41

Binding sites of RNF41 CTD with USP8, TBK1, MYD88, and docking #2 of NSP15

	RNF41-Gly215	RNF41-Met217	RNF41-Thr220	RNF41-Asp222	RNF41-Glu252	RNF41-Arg265	RNF41-Arg269	RNF41-His312
USP8	yes	yes	yes	yes	yes	yes	yes	yes
TBK1	yes	yes	yes	yes	yes	no	no	yes
MYD88	no	yes	no	no	yes	yes	yes	yes
NSP15 (#2)	no	yes	yes	yes	yes	no	yes	yes

Docking results of RNF41 CTD to USP8, TBK1, MYD88, and to the different docking poses of NSP15

Protein	Binding score
USP8	-75.8 +/- 6.6
TBK1	-75.0 +/- 8.8
MYD88	-72.9 +/- 10.6
Docking 1 of NSP15	-91.4 +/- 9.0
Docking 2 of NSP15	-110.9 +/- 3.6
Docking 3 of NSP15	-79.6 +/- 5.6
Docking 4 of NSP15	-40.4 +/- 2.0
Docking 5 of NSP15	-29.4 +/- 10.1

Docking results of RNF41 ZFD to the different docking poses of NSP15

Protein	Binding score
Docking 1 of NSP15	-64.4 +/- 7.0
Docking 2 of NSP15	-50.5 +/- 9.1
Docking 3 of NSP15	-35.7 +/- 2.1
Docking 4 of NSP15	-38.4 +/- 6.0
Docking 5 of NSP15	-29.5 +/- 9.3

NSP15 binds to RNF41 CTD with ~72% greater binding score than when NSP15 binds to RNF41 ZFD, indicating that NSP15 will favor binding to RNF41 CTD. Binding score of NSP15 to RNF41 CTD is ~46% greater than the binding score of USP8 to RNF41 CTD, TBK1 to RNF41 CTD and the binding score of MYD88 to RNF41 CTD. This indicates that RNF41 CTD has a greater binding affinity to NSP15 than RNF41 CTD has to USP8, TBK1, MYD88. If NSP15 binds to the active sites of RNF41, RNF41 will not be able to bind to MyD88 to negatively regulate NF-kB immune signaling pathway. Also, RNF41 will not be able to bind to TBK1 to positively regulate Type 1 Interferon immune signaling pathway. The previously known sites on NSP15 responsible for viral replication are His-236, His-251, Ser-295, Lys-291, Thr-342, Thy-344. They are different from the binding sites of NSP15 with RNF41 CTD and are located ~8 Å away, indicating that viral replication can continue even when NSP15 binds to RNF41 CTD.

MD simulations of 10 ns were processed at 1 atm, 300K, a water box with 10 Å, using OPLS/AA force field under the NPT ensemble with a time step of two femtoseconds (fs) for NSP15 pose#2 docked to RNF41 CTD.

RMSD of backbone of NSP15 docked to RNF41 CTD

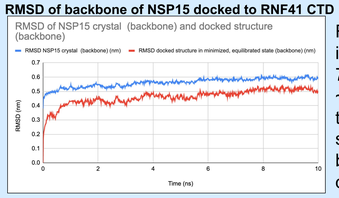

RMSD plots of backbone atoms indicates it reaches stability after 7 ns and RMSD at equilibrium is ~0.51 nm. Comparing the RMSD to that is NSP15 crystal structure shows the RMSD levels are off by ~0.1 nm indicating that the docked structure is stable.

Results and Discussion

RMSD of backbone of the docked structure for NSP15 and RNF41 CTD residues

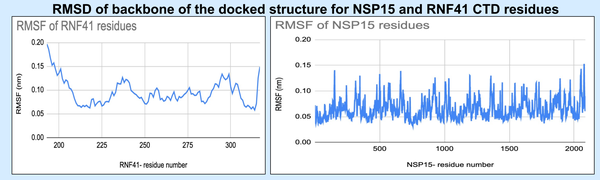

RMSF plots indicated RNF41 and NSP15 have an average RMSF of 0.0644 nm and 0.0955 nm respectively. All RNF41 CTD residues involved in binding exhibited lower than average fluctuations (RMSF value) indicating more stability for the residues in this interaction. Four out of the six residues of NSP15 exhibited fluctuations either closer to or lower than average fluctuations indicating more stability for the residues in this interaction. Two residues of NSP15 involved in the binding, Ser242 and His243, exhibited RMSF values of 0.1113 nm and 0.0936 nm respectively which is greater than the average RMSF of 0.0644 nm indicating slightly lesser stability for these two residues in the interaction.

Rg of backbone of NSP15 docked to RNF41 CTD

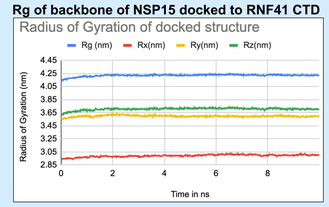

Radius of gyration (Rg) attained a constant value of ~4.2 nm after 2 ns which is close to the average value of 4.22 nm. This indicates that the proteins in the docked structure remain stable and compactly folded during the simulation.

Number of protein-protein hydrogen bonds of NSP15 docked to RNF41 CTD

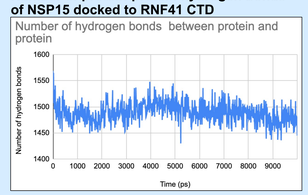

Average number of hydrogen bonds between proteins within 3.5 nm is ~1480. Based on the graph, at different times, the number of hydrogen bonds remain close to the average throughout the 10ns except in the beginning from t=0 ns to to t=0.1 ns where the average number of hydrogen bonds between proteins is ~1520. These results indicate that the complex is stable.

Conclusions

In this ongoing COVID-19 pandemic, in silico methodologies can be used to accelerate the process of understanding the binding interactions of SARS-CoV-2 with human proteins at an atomic level. In this study we used molecular docking to study the binding interactions of SARS-CoV-2 NSP15 and human proteins USP8, MYD88, TBK1, RNF41 CTD, and RNF41 ZFD. The structure of RNF41 ZFD was unavailable in the PDB. So, we used homology modeling to build the previously unknown structure of RNF41 ZFD. Subsequently, we developed a computational algorithm to determined the potential active sites on RNF41 ZFD. Docking results indicated that NSP15 pose#2 had the highest binding affinity to RNF41 CTD. The results also revealed that the active sites on NSP15 that aid in viral replication are different from those where NSP15 binds with RNF41 CTD. Hence NSP15 could continue its function of aiding in viral replication while inhibiting the immune system. Analysis of MD simulations performed on the docked structure of NSP15 and RNF41 CTD indicated that the structure was stable. We validated the hypothesis that NSP15 can bind to RNF41 CTD. This could impair RNF41's function in modulating inflammation and IFN-1 production. The results of our work on binding interactions between the RNF41 CTD and SARS-CoV-2 NSP15 would be useful for further studies, including the designing of efficient antiviral agents that target NSP15.

Funding

This project is partially funded by Department of Energy's National Virtual Biotechnology Laboratory.

Selected References

1. Kim, Youngchang, et al. "Crystal Structure of Nsp15 Endoribonuclease NendoU from SARS-CoV-2." *Protein Science : A Publication of the Protein Society*, U.S. National Library of Medicine, July 2020, www.ncbi.nlm.nih.gov/pmc/articles/PMC7264519/ Accessed July 2020.
2. Li, Shufen, et al. "SARS-CoV-2 Triggers Inflammatory Responses and Cell Death through Caspase-8 Activation." *Nature News*, Nature Publishing Group, 9 Oct. 2020, www.nature.com/articles/s41392-020-00334-0 Accessed October 2020.
3. Meffre, Eric, and Akiko Iwasaki. "Interferon Deficiency Can Lead to Severe COVID." *Nature News*, Nature Publishing Group, 2 Nov. 2020, www.nature.com/articles/d41586-020-03070-1 Accessed November 2020.